Electrical transport properties of Si-doped hexagonal boron nitride epilayers

S. Majety, T. C. Doan, J. Li, J. Y. Lin, and H. X. Jiang[a]
Department of Electrical and Computer Engineering, Texas Tech University, Lubbock, TX 79409, USA

The suitability of Si as an n-type dopant in hexagonal boron nitride (hBN) wide bandgap semiconductor has been investigated. Si doped hBN epilayers were grown via in-situ Si doping by metal organic chemical vapor deposition technique. Hall effect measurements revealed that Si doped hBN epilayers exhibit n-type conduction at high temperatures (T > 800 K) with an in-plane resistivity of $\sim$12 $\Omega \cdot$ cm, electron mobility of $\mu \sim 48$ cm^2/V $\cdot$ s and concentration of n $\sim 1 \times 10^{16}$ cm^{-3}. Temperature dependent resistivity results yielded a Si energy level in hBN of about 1.2 eV, which is consistent with a previously calculated value for Si substitutionally incorporated into the B sites in hBN. The results therefore indicate that Si is not a suitable dopant for hBN for room temperature device applications. *© 2013 Author(s). All article content, except where otherwise noted, is licensed under a Creative Commons Attribution 3.0 Unported License.* [http://dx.doi.org/10.1063/1.4860949]

I. INTRODUCTION

Hexagonal boron nitride (hBN) possesses excellent physical properties such as high thermal conductivity, chemical stability, negative electron affinity, large energy band gap (E$_g \sim$ 6.4 eV), and large neutron capture cross section[1–4] and has been the subject of interest recently due to its potential for various applications. The layered and hexagonal structure is closely lattice matched to graphene making it highly suitable for the construction of hBN/graphene based two-dimensional (2D) heterostructures.[5–7] Lasing action in deep ultraviolet (DUV) region ($\sim$225 nm) by electron beam excitation was demonstrated in small hBN bulk crystals synthesized by a high pressure/temperature (HPHT) technique.[4] This coupled with recent advances in wafer-scale epitaxial growth and the demonstration of extraordinarily efficient band-edge emission brings out its promise as an active DUV photonic material.[8–11] Furthermore, we have shown that it is possible to convert this ultra-wide bandgap material to p-type by Mg doping and a p-type resistivity that is about 6 orders of magnitude lower than Mg doped wurtzite AlN has been measured.[8] This possibility of p-type conductivity control in hBN epilayers represents an exceptional opportunity to revolutionize p-layer approach and overcome the intrinsic problem of low p-type conductivity in Al-rich AlGaN alloys for DUV device applications.[11]

A theoretical calculation indicated that the substitutional Be or Mg incorporated at a B site will act as an acceptor whereas Si or C at a B site as a donor.[12] In fact both p- and n-type conductions have been realized in cubic BN (c-BN) bulk crystals synthesized under HPHT[13–15] The incorporation of Si and S by in-situ doping techniques into c-BN films or films with mixed cBN/hBN phases has also been examined and the microstructures, mechanical properties as well as the field emission characteristics have been studied for these films.[16, 17] To realize devices which require both p-type and n-type hBN materials, n-type conductivity control in hBN is equally important. There have, however, been no reports on the growth and characterization of n-type hBN films. Thus, the effects of Si incorporation in epitaxially grown hBN layers seem worth exploring.

---

[a]hx.jiang@ttu.edu

II. EXPERIMENT

The hBN epilayers were grown using low pressure metal organic chemical vapor deposition (MOCVD) using hydrogen as a carrier gas. The precursors for boron and nitrogen are tri-ethyl boron (TEB) and ammonia (NH_3), respectively. The hBN epilayers were grown on sapphire substrates. A pulsed growth scheme (alternating flows of TEB and NH_3) was undertaken to minimize the pre-reaction between TEB and ammonia, which is important for obtaining epilayers in hexagonal phase. Due to the lattice mismatch between hBN and Al_2O_3, a low temperature BN buffer layer of about 10 nm in thickness grown at 600 °C was deposited on sapphire substrate prior to the growth of hBN epilayer. Without this buffer layer, the adhesivity of hBN layer on top of the substrate is compromised and the epilayer tends to crack more easily. X-ray diffraction (XRD) θ–2θ scan of a representative undoped hBN epilayer ($\sim$0.5 μm) is shown in Fig. 1(a) revealed a c-lattice constant $\sim$6.67 Å, which closely matches to the bulk c-lattice constant of hBN (c = 6.66 Å),[1] affirming that our MOCVD grown films are of single hexagonal phase. Figure 1(b) compares the XRD rocking curves (ω-scans) of the (0002) diffraction peaks of hBN and AlN which has a comparable bandgap as hBN. The observed full width at half maximum (FWHM) of 380 arcsec for hBN is comparable to those of typical GaN epilayers grown on sapphire with a similar thickness,[18] but is much broader than the typical FWHM ($\sim$63 arcsec) of high quality AlN. The results are an indicative of the fact that the development of epitaxial layers of hBN is in its early stage. The grown epilayers also have a good surface morphology as indicated by the SEM image of an hBN epilayer (etched into stripes) shown in the inset of Fig. 1(c). Moreover, as shown in Fig. 1(c), the measured 10 K band edge photoluminescence emission intensity of hBN is more than 2 orders of magnitude higher than that of high quality AlN, originating from the unusually strong $p \to p$-like transitions and its "two-dimensional" nature.[10] Secondary ion mass spectrometry results also revealed that hBN epilayers have excellent stoichiometry.[8] These properties signify that the quality of our MOCVD grown hBN epilayers represents a dramatic improvement over those of previously reported hBN films having XRD rocking curve FWHM of 1.5 °–0.7 °.[19] However, defects including stacking faults and vacancies could all contribute to the broadening of the XRD FWHM. Much work remains to be done to gain in-depth understanding of defect types and mechanisms of their formation and elimination. For the growth of Si doped hBN, silane was transported into the reactor during hBN epilayer growth. The crystalline structure and lattice constant of the Si doped layers were identical to those of undoped layers.

III. RESULTS AND DISCUSSION

The inset of Figure 2 shows the schematic of the layer structure used for the electrical transport studies. Si doped hBN epilayers (hBN:Si) were thermally annealed at high temperatures to improve the electrical conductivity. It was observed that irrespective of the Si concentration, without this annealing process all the samples were highly insulating. We have seen similar effects of post-growth thermal annealing on Mg doped p-type hBN epilayers.[11] After the post-growth thermal annealing, contacts consisting of Ni/Au (30 nm/20 nm) bilayer were deposited using e-beam evaporation. The contacts were then subjected to rapid thermal annealing at 800 °C for 10 minutes to decrease the contact resistance and achieve ohmic characteristics. These processes were adopted from the established GaN device technologies.[20] Figure 2 shows the I-V characteristics of 3 samples grown with different silane flow rates. As can be seen from the plots, Ni/Au bilayers provide excellent ohmic contacts to n-type hBN materials. Furthermore, it can be clearly seen that there is a decrease in resistance with increasing silane flow rate (or equivalently the Si doping concentration) as expected. It is also expected that the material quality and ohmic contact processes will continue to improve with further research works.

Figure 3 compares the I-V characteristics of two hBN:Si samples annealed at (a) T_a = 900 °C and (b) T_a = 1100, measured at different temperatures. The conductivity significantly improved for the hBN:Si epilayer annealed at a higher temperature. However, it was found that annealing the samples above temperatures $>$1100 °C resulted in no further improvements on the electrical conductivity. In order to determine the carrier type, van der Pauw-Hall effect measurements
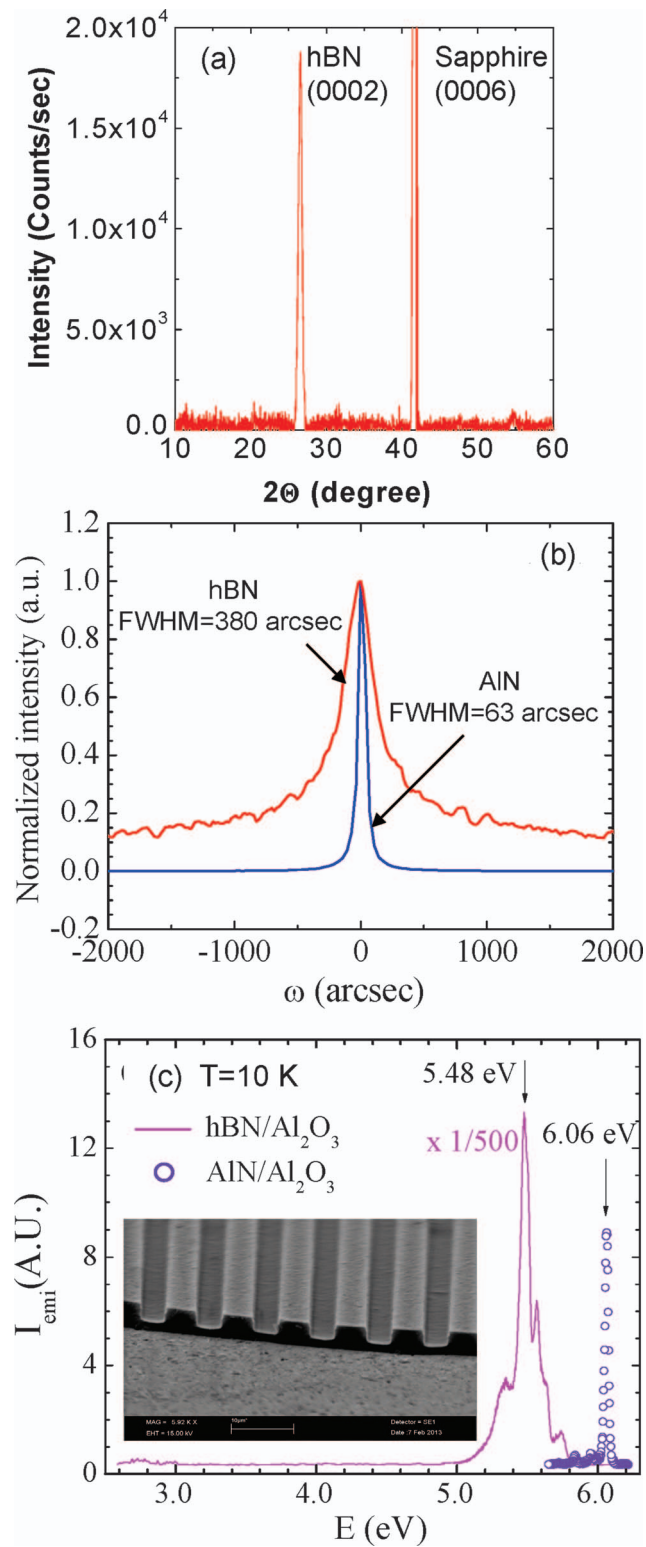
FIG. 1. Basic properties of undoped hBN epilayers grown on sapphire substrates: (a) XRD θ-2θ scan of an hBN epilayer. (b) Comparison of XRD rocking curve of the (0002) diffraction peaks in hBN and AlN epilayers. (c) Comparison of DUV PL spectra of hBN and AlN epilayers measured at 10 K. The inset is the SEM image of an hBN epilayer etched into stripes.
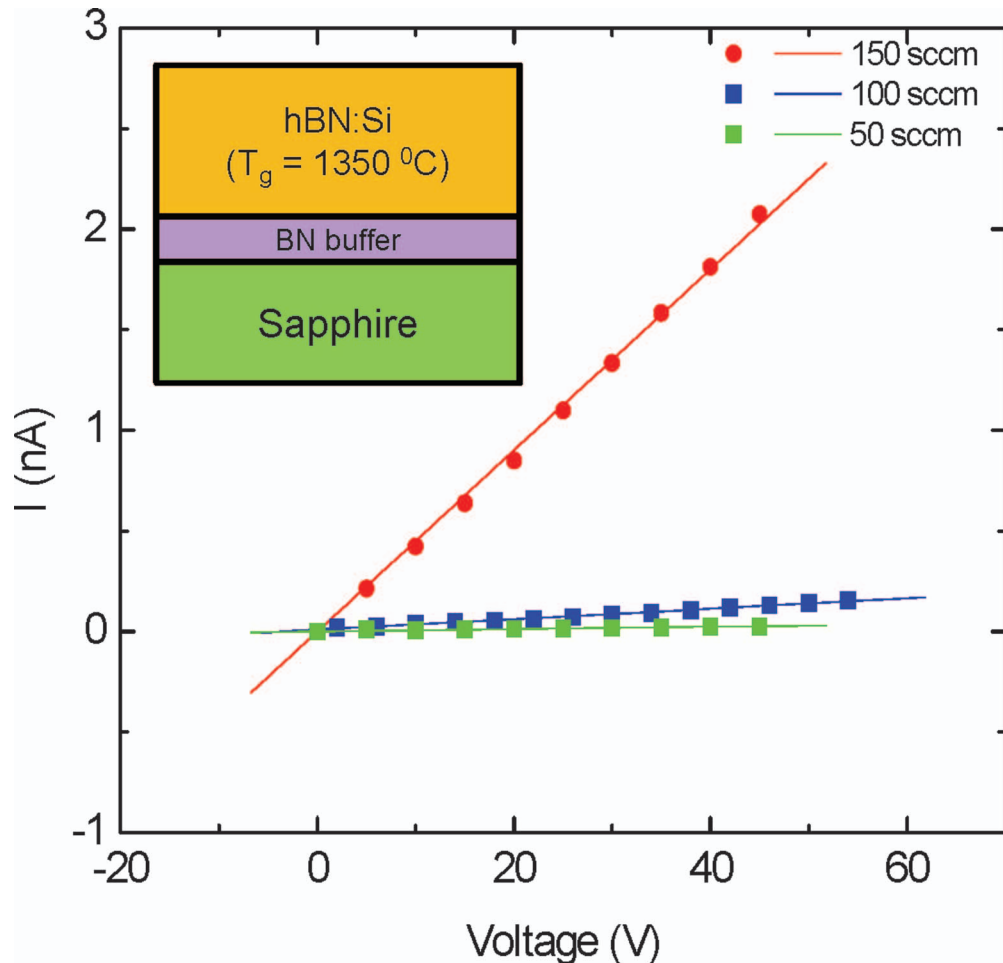
FIG. 2. I–V characteristics of three Si doped hBN epilayer (hBN:Si) samples with different silane flow rates (Si doping concentrations). The inset is the schematic structure of hBN:Si samples used for this study.

were conducted. Since the development of hBN materials is at a very early stage and hBN:Si samples are quite resistive at room temperature, we would like to emphasize that it is important to minimize the impact of macroscopic sample inhomogeneity on the measured carrier type while employing the van der Pauw–Hall method.[21] This can be achieved via the use of square shaped van der Pauw sample geometry with square or triangular ohmic contacts fabricated on the four corners of the sample.[21–23] A recent theoretical study has concluded that "if the ohmic contacts of a square-shaped sample are placed in the corners (and not in the sample interior), the measured carrier type will be correct even in the case of macroscopically inhomogeneous carrier concentrations and/or mobilities".[22] The schematic and microscope image of a fabricated hBN:Si sample and ohmic contact (Ni/Au bilayers) geometry employed for the Hall effect measurements are shown in Fig. 4. The ratio of the contact size (c) to the sample length scale (L) is about 1/5. We thus believe that our van der Pauw sample configuration provides high confidence in the measured carrier type.

Due to the nature of high resistivity of the samples, it was difficult to carry out Hall effect measurements at room temperature and the values of resistivity (ρ), free electron concentration (n) and mobility μ can only be measured at temperatures above 800 K. As illustrated in Fig. 5(a), Hall effect measurements were carried out at 850 K for the sample annealed at $T_a = 1100\,°C$ for multiple times and yielded an average resistivity $\rho \sim 12\ \Omega \cdot cm$ with a free electron density n $\sim 1 \times 10^{16}$ cm^{-3} and mobility $\mu \sim 48\ (\pm 24)$ cm^2/V $\cdot$ s. The mobility data are accompanied by a large fluctuation, however, unambiguously confirmed that hBN:Si exhibits n-type conductivity.

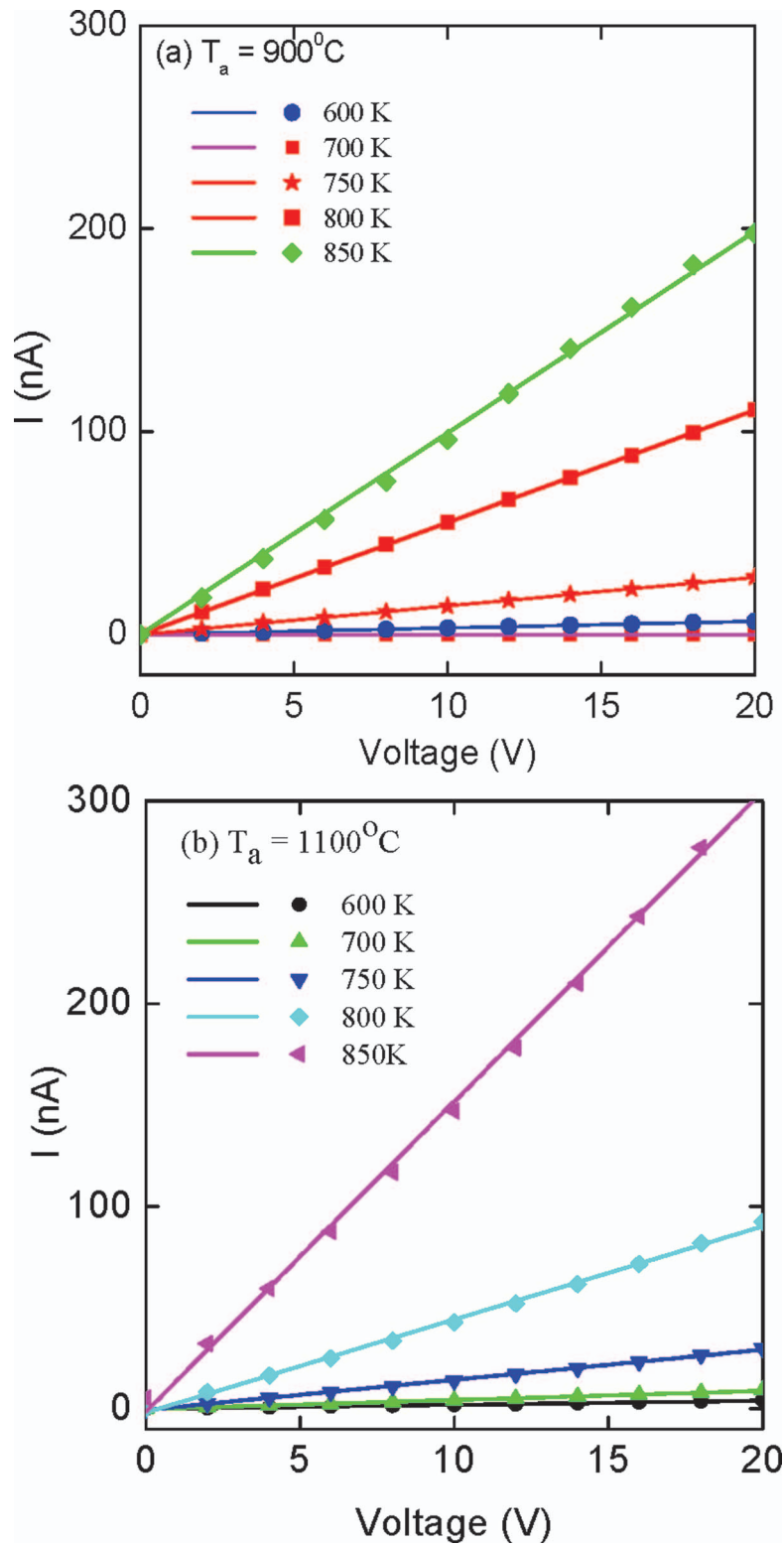FIG. 3. I–V characteristics of hBN:Si samples grown with silane flow rate of 150 sccm, annealed at (a) $T_a = 900\,°C$ and (b) $T_a = 1100\,°C$, measured at different temperatures.
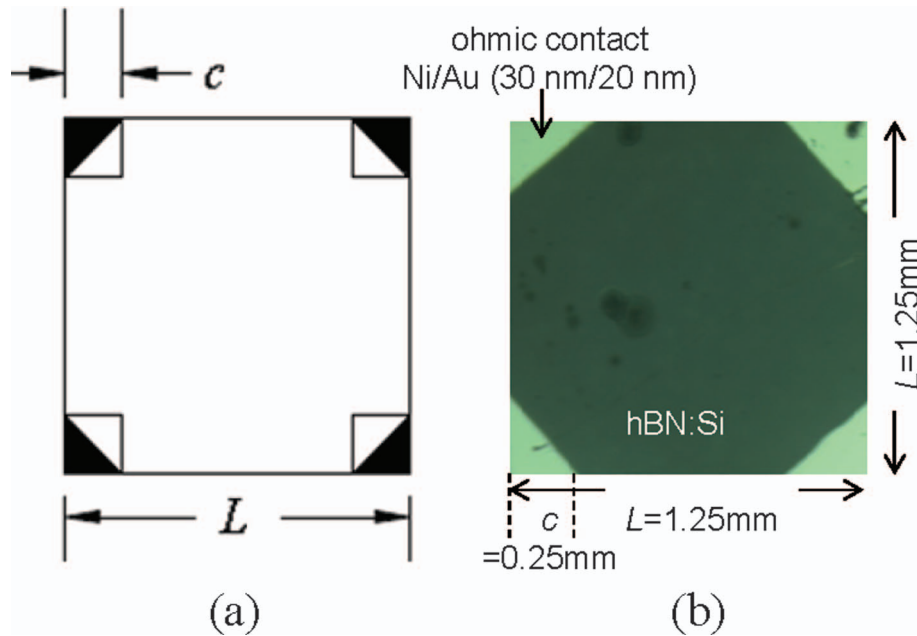
FIG. 4. (a) Schematic and (b) microscope image of a fabricated van der Pauw sample of hBN:Si for Hall effect measurements. The four ohmic contacts on the corners consist of Ni/Au (30 nm/20 nm) bilayers and were deposited using e-beam evaporation followed by rapid thermal annealing at 800 °C for 10 minutes.

In order to deduce the Si donor energy level, the electrical resistances (R) at different temperatures were measured instead of resistivity. Figures 5(b) shows the temperature dependence of R for the sample annealed at $T_a = 1100$ °C. The Si donor energy level (E_D) in hBN:Si can be extracted from the temperature dependent resistances. Neglecting the variation of the mobility with temperature, we have $R \propto \rho \propto 1/n \propto e^{E_D/kT}$ or $R = R_o e^{E_D/kT}$. The Si donor level can thus be obtained by fitting data with the equation:

$$\ln(R) = \ln(R_o) + \frac{E_D}{1000k_B}\frac{1000}{T}. \tag{1}$$

The plot of ln (R) vs 1000/T together with the least squares fitting curve using Eq. (1) is shown in 5(b). The fitted value of E_D for the sample annealed at $T_a = 1100$ °C is ~ 1.19 eV. The measured E_D value is in a close agreement with a previous theoretical calculation,[12] which predicated that E_D would be ~ 1.19 eV if Si atoms were substitutionally incorporated into the B sites.[12] The formation energy of Si-N bond is about 3.98 eV; while the formation energy of Si-B bond is 7.98 eV.[24] Hence Si substituting B is more favorable and more likely to occur than Si substituting N. It is due to such a deep and localized impurity level that Si substitutional dopants are unlikely to have much effects on the electrical properties of hBN and hBN:Si materials are highly insulating at room temperature.

IV. CONCLUSIONS

In summary, Si doped hBN epilayers have been grown via in-situ Si doping by MOCVD technique. High temperature Hall effect and I-V characteristics measurement results indicate that these samples are n-type with an in-plane resistivity of ~ 12 $\Omega \cdot$ cm at 850 K. The measured Si donor energy level is around 1.2 eV and agrees quite well with the calculation results, which implies that Si is not a suitable n-type dopant for hBN for room temperature device applications. Further works are required to understand the mechanisms of conductivity control as well as the choice of dopant species and optimized conditions of post-growth processes of materials, type of metal contacts, and contact annealing conditions.
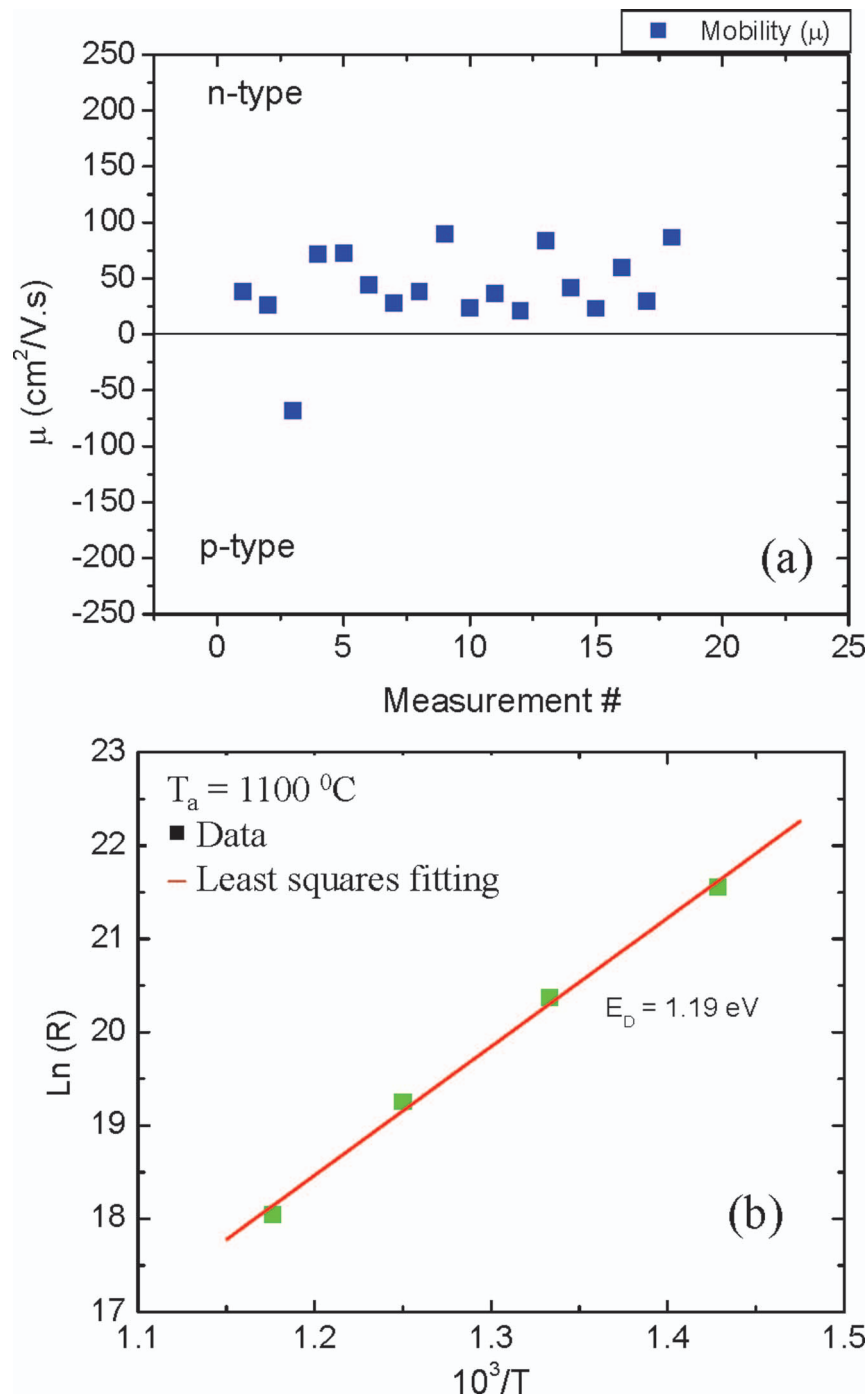
FIG. 5. (a) Mobility data obtained by Hall effect measurements carried out at 850 K for the hBN:Si sample grown with silane flow rate of 150 sccm, annealed at $T_a = 1100\,^\circ$C. In the experimental setup, $+\mu$ means electron conduction and $-\mu$ means hole conduction. The mobility data (measured 18 times) unambiguously confirmed the sample exhibiting n-type conduction. (b) Temperature dependent resistance plotted in the scale of ln (R) vs 1/T for the hBN:Si sample grown with silane flow rate of 150 sccm, annealed at $T_a = 1100\,^\circ$C. The measured Si energy level (E_D) in hBN:Si is also indicated.

ACKNOWLEDGMENTS

[1] S. L. Rumyantsev, M. E. Levinshtein, A. D. Jackson, S. N. Mohammmad, G. L. Harris, M. G. Spencer, and M. S. Shur, in *Properties of Advanced Semiconductor Materials GaN, AlN, InN, BN, SiC, SiGe.* edited by M. E. Levinshtein, S. L. Rumyantsev, and M. S. Shur (John Wiley & Sons, Inc., New York, 2001), p. 67–92.

[2] Y. Kubota, K. Watanabe, O. Tsuda, and T. Taniguchi, Science **317**, 932 (2007).

[3] J. Li, R. Dahal, S. Majety, J. Y. Lin, and H. X. Jiang, Nuclear Instruments and Methods in Physics Research A **654**, 417 (2011).

[4] K. Watanabe, T. Taniguchi, and H. Kanda, Nature Photonics **3**, 591 (2009).

[5] L. Britnell, R. V. Gorbachev, R. Jalil, B. D. Belle, F. Schedin, A. Mishchenko, T. Georgiou, M. I. Katsnelson, L. Eaves, S. V. Morozov, N. M. R. Peres, J. Leist, A. K. Geim, K. S. Novoselov, and L. A. Ponomarenko, Science **335**, 947 (2012).

[6] C. Dean, A. F. Young, L. Wang, I. Meric, G.-H. Lee, K. Watanabe, T. Taniguchi, K. Shepard, P. Kim, and J. Hone, Solid State Communications **152**, 1275 (2012).

[7] A. K. Geim and I. V. Grigorieva, Nature **499**, 419 (2013).

[8] R. Dahal, J. Li, S. Majety, B. N. Pantha, X. K. Cao, J. Y. Lin, and H. X. Jiang, Appl. Phys. Lett. **98**, 211110 (2011).

[9] S. Majety, J. Li, X. K. Cao, R. Dahal, B. N. Pantha, J. Y. Lin, and H. X. Jiang, Appl. Phys. Lett. **100**, 061121 (2012).

[10] B. Huang, X. K. Cao, H. X. Jiang, J. Y. Lin, and S. H. Wei, Phys. Rev. B **86**, 155202 (2012).

[11] S. Majety, J. Li, X. K. Cao, R. Dahal, B. N. Pantha, J. Y. Lin, and H. X. Jiang, Appl. Phys. Lett. **100**, 061121 (2012).

[12] F. Oba, A. Togo, I. Tanaka, K. Watanabe, and T. Taniguchi, Phys. Rev. B **81**, 075125 (2010).

[13] R. H. Wentorf, Jr., J. Chem. Phys. **36**, 1990 (1962).

[14] O. Mishima, J. Tanaka, S. Yamaoka, and O. Fukunaga, Science **238**, 181 (1987).

[15] T. Taniguchi, K. Watanabe, S. Koizumi, I. Sakaguchi, T. Sekiguchi, and S. Yamaoka, Appl. Phys. Lett. **81**, 4145 (2002).

[16] T. Sugino, K. Tanioka, S. Kawasaki, and J. Shirafuji, Jpn. Appl. Phys. **36**, L463 (1997).

[17] J. Ying, X. W. Zhang, Z. G. Yin, H. R. Tan, S. G. Zhang, and Y. M. Fan, J. Appl. Phys. **109**, 023716 (2011).

[18] S. Nakamura, G. Fasol, and S. J. Pearton, *The Blue Laser Diode: The Complete Story* (Springer, New York, 2000).

[19] Y. Kobayashi, T. Akasaka, and T. Makimoto, J. Cryst. Growth **310**, 5048 (2008).

[20] S. J. Pearton, J. C. Zolper, R. J. Shul, and F. Ren, J. Appl. Phys. **86**, 1 (1999).

[21] L. J. Van der Pauw, Philips Research Reports **13**, 1 (1958).

[22] O. Bierwagen, T. Ive, C. G. Van de Walle, and J. S. Speck, Appl. Phys. Lett. **93**, 242108 (2008).

[23] A. Kumar, J. Pernot, F. Omnès, P. Muret, A. Traoré, L. Magaud, A. Deneuville, N. Habka, J. Barjon, F. Jomard, M. A. Pinault, J. Chevallier, C. Mer-Calfati, J. C. Arnault, and P. Bergonzo, J. Appl. Phys. **110**, 033718 (2011).

[24] M. S. Si and D. S. Xue, Europhys. Lett. **76**, 664 (2006).